YALE JOURNAL OF BIOLOGY AND MEDICINE 97 (2024), pp.153-164. doi: 10.59249/EWOI2166

ORIGINAL CONTRIBUTION

YALE JOURNAL OF BIOLOGY AND MEDICINE
YJBM

Therapeutic Potential of Nitrogen-Doped Rutin-Bound Glucose Carbon Dots for Alzheimer's Disease

Sana Khan[a], Faria Hasan Jatala[a], Alveena Muti[a], Noor Afza[a], Aneeqa Noor[a,*], Sara Mumtaz[b], and Saima Zafar[a,c]

[a]*School of Mechanical and Manufacturing Engineering (SMME), National University of Sciences and Technology (NUST), Islamabad, Pakistan;* [b]*Department of Biological Sciences, National University of Medical Sciences, Rawalpindi, Pakistan;* [c]*Clinical Department of Neurology, University Medical Center Göttingen and the German Center for Neurodegenerative Diseases (DZNE), Göttingen, Germany*

The blood-brain barrier (BBB) prevents the use of many drugs for the treatment of neurological disorders. Recently, nitrogen-doped carbon dots (NCDs) have emerged as promising nanocarriers to cross BBB. The primary focus of our study was to evaluate the effectiveness of NCDs for the symptomatic treatment of Alzheimer's disease (AD). In this study, we developed and characterized NCDs bound to rutin, a flavonoid with known benefits for AD. Despite its benefits, the transportation of rutin via NCDs for AD therapy has not been explored previously. We characterized the particles using FTIR and UV-visible spectroscopy followed by atomic force microscopy. Once the design was optimized and validated, we performed *in vivo* testing via a hemolytic assay to optimize the dosage. Preliminary *in vitro* testing was performed in AlCl3-induced rat models of AD whereby a single dose of 10 mg/kg NCDs-rutin was administered intraperitoneally. Interestingly, this single dose of 10 mg/kg NCDs-rutin produced the same behavioral effects as 50 mg/kg rutin administered intraperitoneally for 1 month. Similarly, histological and biomarker profiles (*SOD2* and *TLR4*) also presented significant protective effects of NCDs-rutin against neuronal loss, inflammation, and oxidative stress. Hence, NCDs-rutin are a promising approach for the treatment of neurological diseases.

INTRODUCTION

In 2018, it was estimated by Alzheimer's Disease International that approximately 50 million individuals globally are affected by dementia, with a projected tripling of this figure by 2050, with two-thirds of cases being reported in low- and middle-income countries [1]. Alzheimer's disease (AD) has emerged as a major challenge to public health, due to the augmented longevity of life of the general populace and a more comprehensive

*To whom all correspondence should be addressed: Dr. Aneeqa Noor: Email: aneeqa_n@yahoo.com, Aneeqa.noor@smme.nust.edu.pk. ORCID: 0000-0001-8692-3161.

Abbreviations: BBB, blood-brain barrier; NCDs, nitrogen-doped carbon dots; AD, Alzheimer's disease; NFTs, Neurofibrillary tangles; NPs, Nanoparticles; Aβ, Amyloid beta; *SOD2*, superoxide dismutase; *TLR4*, Toll-like receptor 4; GQDs, Graphene Quantum Dots; CDs, Carbon Dots; CNS, central nervous system; UV-Vis, Ultraviolet-Visible; AFM, Atomic Force Microscopy; FTIR, Fourier transform infrared radiation; NOR, Novel object recognition test; MWM, Morris water maze test; RT-PCR, Real-time Polymerase Chain Reaction.

Keywords: Carbon dots, rutin, Alzheimer's disease, neurodegeneration

Author Contributions: Design: SK, AN, SZ. Data Collection: SK, FHJ, AM, NA. Compilation of Results: All authors. Preparation of manuscript: All authors.

Copyright YJBM © 2024

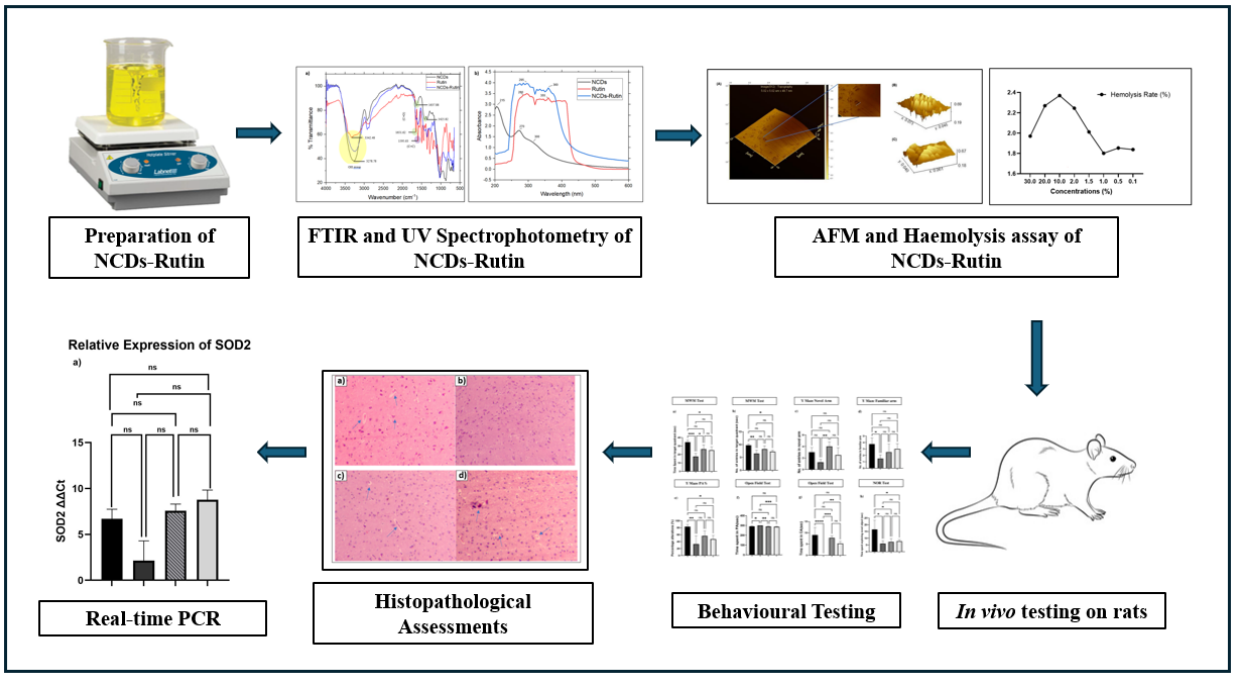

Graphical abstract. In this study, NCDs-rutin carbon dots were prepared and characterized using FTIR, UV Spectrophotometry, and AFM for structural analysis. Hemolysis assay was performed to detect the rate of cell lysis. Supplementarily, *in vivo* testing was also performed, followed by histopathological assessments and RT-PCR.

understanding of the socio-economic implications of the ailment. Alois Alzheimer delineated AD in the year 1906, utilizing criteria of disorientation, progressive cognitive impairment, and pathological markers like senile plaques and neurofibrillary tangles (NFTs) [2]. The early manifestation of AD can be attributed to the deposition of Amyloid beta (Aβ) peptide in the form of amyloid plaques in the brain, leading to neurodegeneration that results in cognitive and functional impairment [3].

Alongside amyloid plaques, intracellular NFTs including hyperphosphorylated tau protein are another neuropathological marker of AD. Current disease models suggest that tau pathology is triggered by Aβ, and at a later stage, a complex and synergistic relationship between Aβ and tau emerges leading to mitochondrial dysfunction, oxidative stress, inflammation, and neuronal loss [4]. The primary enzyme that plays a role against the deleterious molecules associated with stress is the superoxide dismutase (*SOD2*). It efficiently transforms superoxide (harmful radicals) into a less reactive hydrogen peroxide (H_2O_2), which has the ability to permeate through the mitochondrial membrane unhindered [5]. The maintenance of redox equilibrium and the protection of neuronal cells from oxidative damage rely on the signaling of *SOD2*. An elevation in superoxide radical levels could stem from malfunctioning *SOD2* activity, leading to an escalation of oxidative stress and furthering neuroinflammation [6]. Additionally, Toll-like receptor 4 (*TLR4*), a receptor involved in recognizing pathogen-associated molecular patterns and damage-associated molecular patterns, plays a crucial role in the immune response [7]. Expressed on microglia, astrocytes, and neurons in the brain, *TLR4* identifies both internal and external ligands contributing to the process of neuroinflammation [8]. Studies have indicated that Aβ interacts with *TLR4*, activating the MAPK and NF-κB signaling pathways and inducing the production of proinflammatory molecules like IL-1β, IL-6, and TNF-α [9]. Despite decades of research, the field is yet to find effective medicinal interventions to limit the progression of AD.

The blood-brain barrier (BBB), characterized by its predominantly semipermeable nature, poses a significant obstacle to the delivery of treatment medicines for brain disorders [10,11]. The key advantage of utilizing smart nanoparticles (NPs) is their ability to respond to both internal and external stimuli in predictable and specific ways, which enhances the control of delivery process. Additionally, research has demonstrated that the covalent coupling of NPs and various ligands can significantly improve the efficacy of drug delivery [12]. Carbon nanomaterials, a fresh classification of carbon-based substances, consisting of nanodiamonds, fullerenes, graphene quantum dots (GQDs), carbon dots (CD), and carbon nanofibers, have garnered significant attention in the realm of nanotechnology. The most recent addition to this family, with a magnitude less than 10 nm, is the CD. Due to their

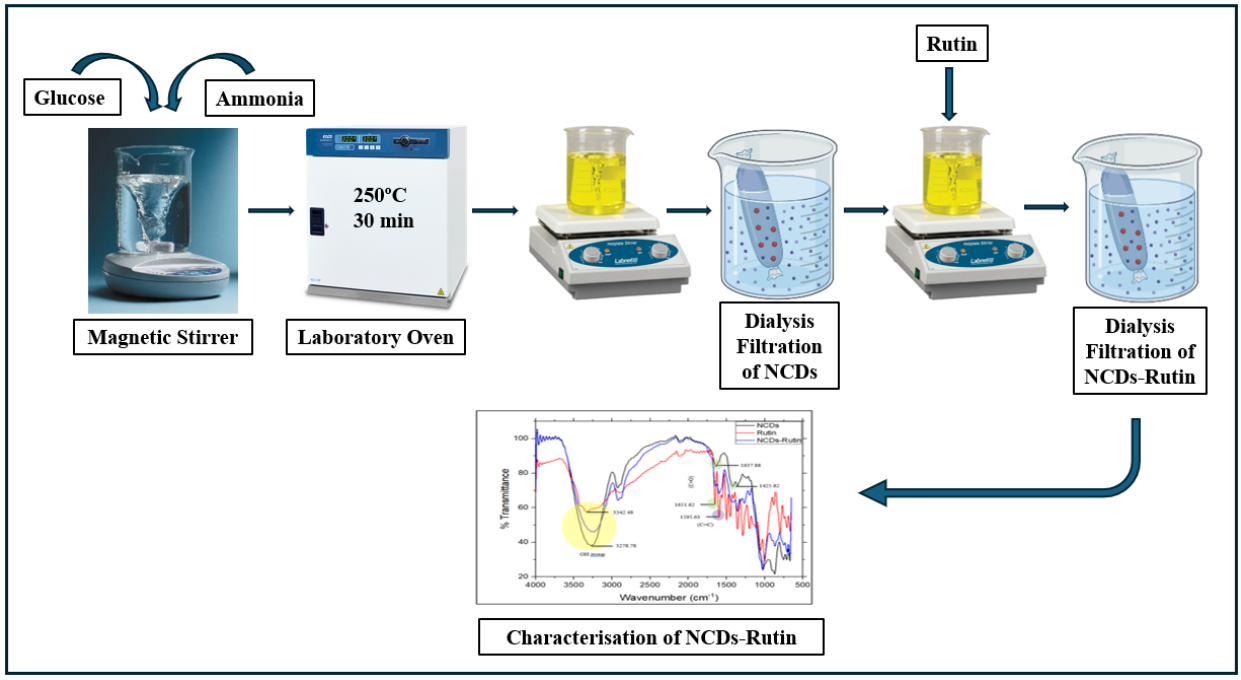

Figure 1. **Preparation of NCDs-rutin**. A mixture of glucose, water, and ammonia was heated in the laboratory oven at 250°C. To remove any unbound molecules, dialysis filtration is performed. After the addition of rutin and overnight stirring, dialysis filtration is performed again to filter out any unbound particles. The resulting NCDs-rutin is then lyophilized before characterization.

distinctive properties, encompassing exceptional photoluminescence (PL), high biocompatibility, abundance of surface functional groups, non-toxicity, and nanoscale dimensions, CDs are among the most auspicious candidates for BBB penetration [13-15]. CDs have exhibited their ability to traverse the BBB. Furthermore, the surfaces of CDs are endowed with abundant amine (-NH2) and carboxyl (-COOH) groups, which can be leveraged to couple with diverse central nervous system (CNS) pharmaceuticals. Additionally, CDs are biocompatible, rendering them suitable for biological therapeutics. For the treatment of AD and brain tumors, CDs serve as exceptional nanocarriers for delivering drugs into the CNS. One of the most widely used treatments for AD involves lowering the deposition of Aβ in the CNS [16].

Traditional medicinal practices have embraced a multitude of herbal remedies in treating various ailments since ancient times. These remedies, apart from serving as a source of nutrition, have proven to be effective in curing a range of disorders [17]. In comparison to pharmaceuticals, certain plant extracts have demonstrated superior performance while being less toxic and having fewer side effects [18]. The therapeutic characteristics of plants can be attributed to the presence of flavonoids, glycosides, tannins, alkaloids, terpenoids, and other secondary metabolites. The potential for rutin (3,3′,4′,5,7-pentahydroxyflavone-3-rhamnoglucoside), a hydrophobic natural flavonoid, to be delivered through CDs was explored in this study [19]. Rutin demonstrates a diverse range of pharmacological effects and can be employed to treat a broad spectrum of ailments such as diabetes, hypertension, cancer, and hypercholesterolemia. Moreover, it is known for its cytoprotective, antibacterial, antioxidant, anticarcinogenic, vasoprotective, neuroprotective, and cardioprotective properties [20].

Although rutin holds several benefits for the symptomatic treatment of AD, its limited water solubility and cell permeability greatly impede its potential to induce pharmacological effects [21]. To overcome these restrictions, the current study demonstrates the use of NCDs as a drug transporting vehicle to enhance the pharmacological activities of this medication with relevance to AD.

MATERIALS AND METHODOLOGY

Ethical Approval

Before conducting this study, ethical approval (IRB no. 05-2023-ASAB-02/02) was acquired from the Institutional Review Board of the National University of Sciences and Technology, Islamabad, Pakistan.

Chemicals

Glucose (BCCF4025, Sigma Aldrich, Switzerland),

Ammonia (10314944, Honeywell, Germany), Rutin hydrate (207671-50-9, Macklin, China), dialysis membrane (500 Da cut off, MD55, Scientific Research Special, China), Phosphate Buffered Saline (2810305, MP Biomedicals, France), Dimethyl sulfoxide (67-68-5, Sigma Aldrich, Switzerland), and Ultrapure Millipore water (7732-18-5, Sigma Aldrich, Switzerland), and Sodium hydroxide (NaOH) were purchased from a local vendor.

Preparation of NCDs

Using the uniform heating technique, NCDs were prepared by dissolving 5 g of glucose in 50 ml of water. Following vigorous swirling, 2.5 ml of ammonia was added to the aforementioned solution. The resulting translucent mixture was subjected to a temperature of 250°C for a duration of 30 minutes in a laboratory oven. The color transition of the sample from translucent to pale yellow is indicative of the presence of NCDs. To ensure the complete elimination of any remaining ammonia, the pale yellow solution was rapidly agitated for 1 hour after being chilled. After that, pH 7 was attained by adding NaOH/HCl solution dropwise using a basic pH meter. To eliminate residual unfused small and large molecules, the aqueous solution of NCDs underwent a dialysis process against Millipore water for a duration of 48 hours using a dialysis membrane [22].

Preparation of NCDs-Rutin

The dissolution of rutin in Dimethyl sulfoxide (DMSO) was amalgamated with the aqueous CD solution using a mass ratio of 1:1. Stirring was performed at room temperature throughout the night while rutin was being loaded. The resulting solution was subsequently dialyzed for 2 hours to remove any unbound molecules. To acquire NCDs-rutin in the form of powder, the purified, drug-loaded NCDs were subjected to lyophilization [23]. Figure 1 briefly summarizes the preparation process of NCDs-rutin.

Characterization of NCDs-Rutin

The morphological structure and chemical composition of prepared NCDs were characterized using different techniques, ie, Ultraviolet-Visible (UV-Vis) Spectroscopy, Atomic Force Microscopy (AFM), and Fourier transform infrared radiation (FTIR) spectroscopy.

FTIR Spectroscopy

FTIR (Agilent Cary 630, Agilent Technologies, USA) has been employed to detect the functional groups present on the surface of NCDs. The bonds and functional groups in the sample were analyzed by FTIR spectroscopy in a range of 500-4000 cm^{-1} at 4 cm^{-1} resolution.

UV-Vis Spectroscopy

UV-visible absorption spectrophotometer (UV-1602, BMS, Germany) with a resolution of 1 nm between the range of 200 and 600 nm was used.

AFM

AFM investigations were conducted using a commercial silicon tip (RTESPA 300, Bruker, USA) with a resonance of 300 kHz and nominal elastic constant of 40 Nm^{-1} on a Multimode 8 Bruker AFM microscope equipped with a Nano scope V controller. The ScanAsystTM was utilized with a scan size of 3 mm.

Hemolytic Assay

The hemolytic assay was implemented as a means of evaluating compatibility with blood by utilizing a microplate reader (Thermo Scientific™ Multiskan™ Sky), the absorbance was measured at 577 nm [24].

Animal Testing

Adult male Albino rats (n = 16) were purchased and housed in the animal house of Atta-ur Rahman School of Applied Biosciences (ASAB), National University of Sciences & Technology (NUST), Islamabad, under controlled environmental conditions (25 ± 2°C). Natural light and dark cycles (14 h light and 10 h dark) were followed. Feed and water *ad libitum* were provided to the animals. They were divided into four groups where n = 4 in each group. Group 1 was the control group, Group 2 was the diseased group, 3 was the NCDs-rutin treated group, and 4 was the rutin group. Groups 2, 3, and 4 were treated with $AlCl_3$ for 15 days. $AlCl_3$ was used to develop diseased models instead of transgenic animals due to the short time taken in development of behavioral alterations. Additionally, the ease of availability and affordability of $AlCl_3$ are attractive merits. After the validation of disease induction, NCDs-rutin treated group was then administered one 10 mg/kg dose of rutin-bound NCDs, while rats of Group 4 were treated with rutin (50mg/kg) intraperitoneally for 1 month; PBS was used as a vehicle [25]. NCDs-rutin dose was determined by conducting *in vitro* hemolytic assay and considering the studies conducted previously [24].

Behavioral Testing

Behavior tests were performed on the 16th day of the $AlCl_3$ treatment and 1 week after administering the NCDs-rutin dose. A total of four behavioral tests were conducted using standardized protocols, ie, Novel object recognition test (NOR), Open field Test, Morris water maze test (MWM), and Y maze test [26,27].

Table 1. List of Primers Utilized in the Current Study

Gene	Direction	Length	Sequence (5 to 3)	Annealing Temp (˚C)
β-Actin	Forward	19	CATCCCCCAAAGATTCTAC	57
	Reverse	17	CAAAGCCTTCATACATC	
Superoxide dismutase 2 (SOD2)	Forward	22	CAGACCTGCCTTACGACTATGG	66
	Reverse	21	CTCGGTGGCGTTGAGATTGTT	
Toll-like receptor 4 (TLR4)	Forward	20	GTGGGTCAAGGACCAGAAAA	66
	Reverse	19	GAAACTGCCATGTCTGAGCA	

The table shows the forward and reverse primers of β-Actin, *SOD2*, *TLR4* with their specific length, sequence, and optimized annealing temperature.

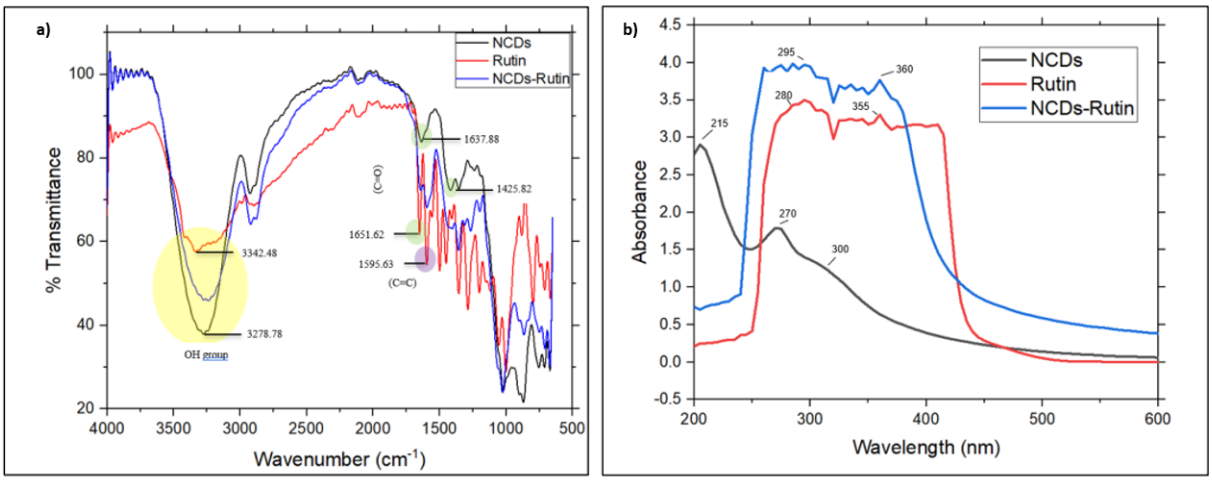

Figure 2. **Characterization techniques performed on NCDs-rutin** (**a**) FTIR spectra of NCDs, rutin, and NCDs-rutin. The black line depicts the IR spectra of simple NCDs, red represents the rutin, while blue shows rutin-bound NCDs. The yellow highlighted area depicts the presence of OH groups in the compounds. Green represents the C=O bond and purple shows the C=C bond (**b**) UV-Vis spectrum of NCDs, rutin, and NCDs-rutin. The UV spectra depict the peaks of NCDs (black) at 215 nm, 270 nm, and 300 nm, rutin (red) at 280 nm and 355 nm; and NCDs-rutin (blue) at 295 nm and 360 nm.

Histopathological Assessments

Hematoxylin and Eosin staining was performed on 5μ tissue sections, and the slides were imaged using a Labomed microscope (Labo America Inc. USA). Image analysis was performed using ImageJ (version 1.53) software [28,29].

Real-time Polymerase Chain Reaction (RT-PCR)

The male Albino rats were deeply anesthetized and euthanized. The brain was removed, snap-frozen on dry ice, and kept at -80°C for later processing. The total RNA from the tissues was isolated using the TRIzol isolation reagent (Catalog No: FTR100, Fine Biotech Life Sciences, China) followed by cDNA synthesis using RevertAid Reverse Transcriptase (Catalog No: EP0441, Thermo Fisher Scientific, Lithuania). To determine the relative expression of the rat genes *SOD2* and *TLR4*, each experimental group underwent RT-PCR using the WizPure™ qPCR Master (SYBR) on a RT-PCR detection system normalized to the expression of beta-actin as a housekeeping gene. The values obtained were analyzed and gene expression was evaluated using ΔCt values (Table 1).

Statistical Analysis

Data visualizations and statistical analysis were conducted using Graph Pad Prism software 10. Error bars present SEM (*p<0.05, **p<0.01, ***p<0.001). One-way ANOVA, followed by Tukey's multiple comparison tests, was used for statistical analysis of all the tests.

RESULTS

Characterization

FTIR Analysis: FTIR analysis indicates the presence of hydroxyl, carboxyl, and carbonyl groups on the sur-

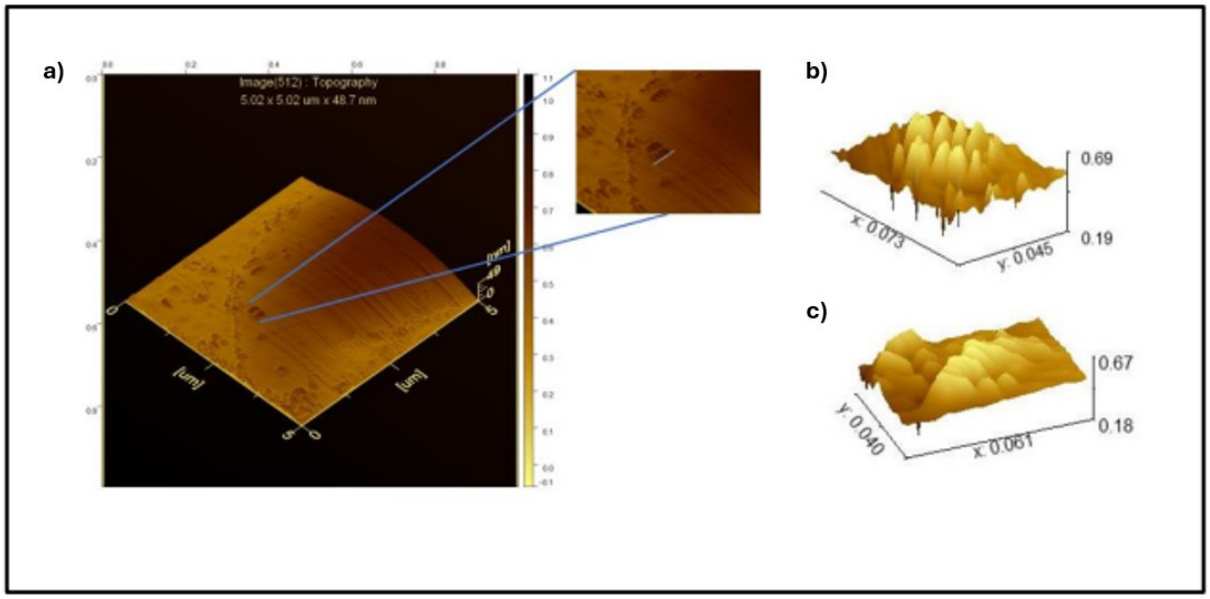

Figure 3. **AFM results for NCDs-rutin, depicting topography**. The figure shows the particle aggregates on a 1 cm glass slide, with an enlarged image of a specific area where particles can be observed (**a**). Images (**b**) and (**c**) exhibit 3D images of the enlarged area depicting the height and thickness of the NCDs-rutin particles.

face edges of NCDs, thereby confirming their exceptional stability and water dispersibility (Figure 2a; [30]). They displayed an absorption peak at 1637.88 cm^{-1} (C=O) and 1425.82 cm^{-1} (C-H), which corresponds to the C-H symmetric stretching vibration [31]. The IR absorption peak for hydroxyl (O-H) was observed at 3278.78 cm^{-1} and the vibration region C=N stretching was noted at 1630 cm^{-1}. The vibrational frequency of the important v(C=O) bond in rutin was discovered to be 1651.62 cm^{-1}. Notably, the benzene ring skeleton in rutin exhibits v(C=C) stretching bonds at 1595.63 cm^{-1}. The stretching vibrations of the OH/H2O groups were observed as wide bands at 3342.48 cm^{-1}. NCDs-rutin depicted a peak at 3266.48 cm^{-1} and 1593.16 cm^{-1} corresponding to the original samples showing OH groups and C=C bonds.

UV-Vis Spectrophotometry: The UV-Vis spectra of NCDs (Figure 2b) exhibited distinct absorption peaks at 215 nm, 270 nm, and 310 nm. Rutin exhibits two absorption bands, specifically at 360 nm (band I) and 295 nm (band II). This observation is consistent with the results from the study conducted previously [32]. NCDs-rutin showed similar peaks to rutin at 295 nm and 355 nm. The aforementioned bands can be attributed to the $\pi - \pi*$ transition of a benzene ring-conjugated system.

AFM Analysis: The morphology of the synthesized NCDs and NCDs-rutin was examined using AFM, as depicted in Figure 3. The results revealed the existence of <100 nm-sized minute aggregates and individual NCDs-rutin particles. Notably, the height observed of NCDs-rutin is 49 nm and the average size is 25 ± 2 nm. The resulting height and diameter profile correspond to the size of particles that can cross the BBB, ie, between 0-200 nm.

Hemolytic Test: Different concentrations of the NCDs-rutin were assessed via hemolytic assay (Figure 4). The hemolysis rates of NCDs-rutin were observed to be substantially lower than the universally recognized standard of 5%, across a concentration range of 0.1% to 30% [33]. The hemolysis rate decreased from 10% to 1% and showed a slight increase in 1.5% and 2% concentrations. The excellent biocompatibility and fulfilment of hemolysis rate prerequisites by the NCDs-rutin, signify their potential for implementation in biological applications.

Behavioral Tests

MWM Test: The results of the escape latency test indicated that the treated rats exhibited a slightly reduced latency in reaching the platform in comparison to the diseased group (Figure 5a). However, the treated rats exhibited slightly significant results with a p-value <0.05, in the duration spent in the target quadrant, whereas the results were nonsignificant in the number of entries. The rats administered with rutin treatment showed a slightly reduced latency to reach the platform when compared to the disease group, according to the results of the escape latency test. Similarly, the number of entries and the duration that treated rats spent in the target quadrant showed promising differences (Figure 5b and 5c). NCDs-rutin yielded p <0.05, indicating slightly significant results in comparison to diseased rats.

Y Maze Test: Only the parameter of time spent in the

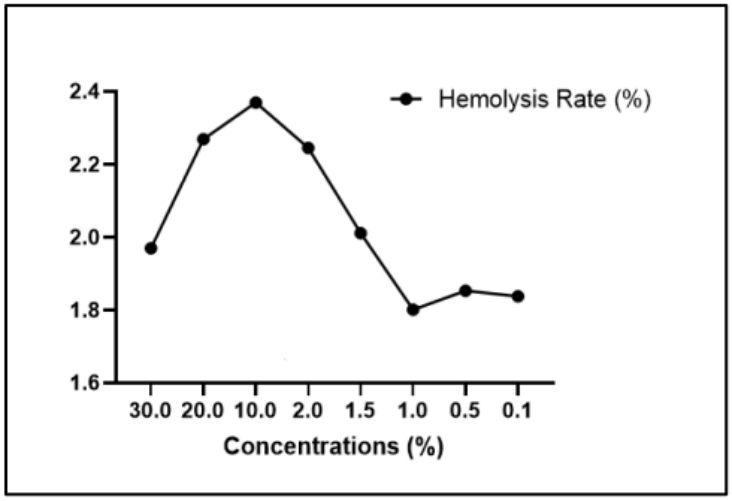

Figure 4. **Hemolysis rate (%) of RBCs treated with different concentrations of NCDs-rutin**. The OD was checked on 577 nm. Deionized water was used as positive control whereas PBS was used as negative control in this experiment. All the rates lie below 5%, which is as per universally recognized standards [33].

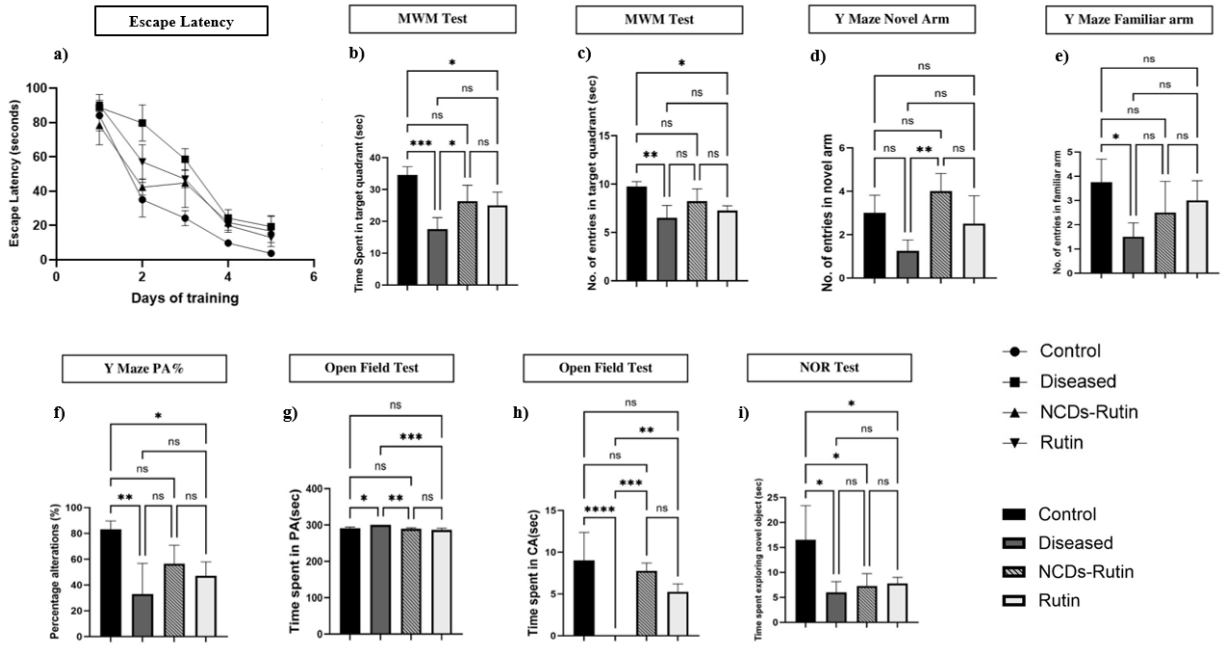

Figure 5. **Behavioral tests after NCDs-rutin administration**: In MWM test, the escape latency (**a**), time spent in target quadrant (**b**) and number of entries in target quadrant (**c**) were observed to be improved in treated groups. The NCDs-rutin group demonstrated higher number of entries in the novel arm and lower number of entries in the familiar arm than in the rutin group in the Y-maze test (**d** and **e**). Percentage of alteration was also observed (**f**). The time spent in the peripheral area and time spent in the central area was increased in both treatment groups compared to the disease group in an open field test (**g** and **h**). In the NOR test, both treatment groups showed statistically no significant results compared to the disease group and also when compared with each other (**i**). Error bars present SEM (*p<0.05, **p<0.01, ***p<0.001). One-way ANOVA, followed by Tukey's multiple comparison tests, was used for statistical analysis of all the tests.

novel arm showed significant differences among the diseased and treated groups ($p < 0.01$), while the other two did not. It is noteworthy that the treated group did show recovery trends in alterations and entries in the familiar arms (Figure 5d and 5e). It was observed that the percentage of alterations (Figure 5f), number of entries in the familiar arm, and number of entries in the novel arm showed increased levels in rutin treated group but not a significant result in all three arms when compared with the control and diseased group.

Open Field Test: Treated rats were observed to spend more time in the central area than the diseased rats while exploring the field (Figure 5g), yielding a p value <0.001, indicating highly significant results. Whereas diseased rats spent the whole time in the peripheral area (Figure 5h).

NOR Test: The results of the test conducted to assess the rats' ability to recall object position or identification, showed no significant difference between the treated and the diseased group (Figure 5i). While both groups displayed similar patterns of exploratory behavior, the treated rats exhibited slightly more inclination to jump onto the objects. The test results, which evaluated the rats' memory for item position or identification, revealed a significant difference between the treated and diseased groups. The two groups of rats showed distinct exploratory activity patterns, with the treated rats showing a somewhat higher propensity to leap onto the items.

Histopathological Analysis

After the intervention of NCDs-rutin, lesser neuronal loss was observed. This suggests positive role of NCDs-rutin in preventing neuronal loss associated with AD (Figure 6). A similar trend was observable for the rutin group, although the protective effect was more profound in response to NCD administration.

Relative Expression of Biomarkers

The relative expression of *SOD2* and *TLR4* is shown in Figure 7. The relative mRNA expression of genes of interest was measured and normalized to the expression of β-actin as a housekeeping gene. Administration of $AlCl_3$ decreased the expression levels of *SOD2* indicating oxidative damage. After NCDs-rutin and rutin administration, *SOD2* levels were found to be up-regulated (fold change depicted with relevance to disease group). On the contrary, $AlCl_3$ administration yielded increasing expression levels of *TLR4.* Following NCDs-rutin and rutin administration, the relative expression level of *TLR4* significantly decreased with $p < 0.05$ and $p < 0.01$ respectively (fold change depicted with relevance to control group). However, the direct comparison between NCDs-rutin and rutin showed no significant difference in the expression levels of *SOD2* and *TLR4* mRNA.

DISCUSSION

Recent advancements in nanoparticle technology, particularly in nanoparticle-mediated drug transport, have made substantial progress in overcoming the BBB. The manifold surface molecules of CDs offer immense potential for conjugation with one or more ligands, serving as CD-based drug delivery systems (DDS) capable of penetrating the BBB to remedy neurological conditions and brain tumors [34]. Currently, most proposed processes lack thorough analysis. To achieve enhanced solutions for the persistent challenges associated with CNS medication delivery, comprehension of these intricate systems is imperative. As drug components, natural flavonoids such as rutin can be utilized to bind to the CDs and can exhibit synergistic effects against AD. In order to enhance rutin's bioavailability, the current study was carried out wherein we hypothesized that loading rutin on a molecule that is small enough and recognized by the BBB for easier passage will yield amplified effects at the target area. Rutin's neuroprotective qualities primarily entail the activation of the MAPK pathway and the inhibition of apoptosis, which is induced by Aβ oligomers [35]. Rutin also amplifies the activity of several enzymes with antioxidant properties, such as *SOD2*, Catalase, and Inhibitor of iNOS Activity [36]. The present study focuses on the production and characterization of rutin-bound NCDs. The prepared NCDs-rutin complex was characterized using FTIR, UV-Vis Spectrophotometer, and AFM, for structural analysis.

In the current study, the water dispersibility of NCD-rutin was confirmed through FTIR analysis that revealed the existence of hydroxyl and carboxyl functional groups. The peaks of these groups are similar to the findings of Sharma and Kunjiappan [22,37]. Similarly, the peaks in the UV spectroscopy coincide with the peaks in the previous work [22,38]. NCDs-rutin showed similar peaks to rutin at 295 nm and 355 nm, attributing to the $\pi - \pi*$ transition of a benzene ring-conjugated system. AFM indicated the average size of the particle to be 25 ± 2 nm, which corresponds to the study by Betzer in which they concluded that particle size of 20-70 nm depicted sufficient accumulation in the brain [39]. The hemolysis rates of NCDs-rutin were observed to be substantially lower than the universally recognized standard of 5%, across a concentration range of 0.1% to 30%, depicting good biocompatibility of the complex material [24].

In addition to characterizing and *in vitro* testing of NCDs-rutin, a supplementary *in vivo* test was also performed. Using behavioral assays, cognitive conditions before and after administration of NCDs-rutin were determined. A range of cognitive tests are available for the as-

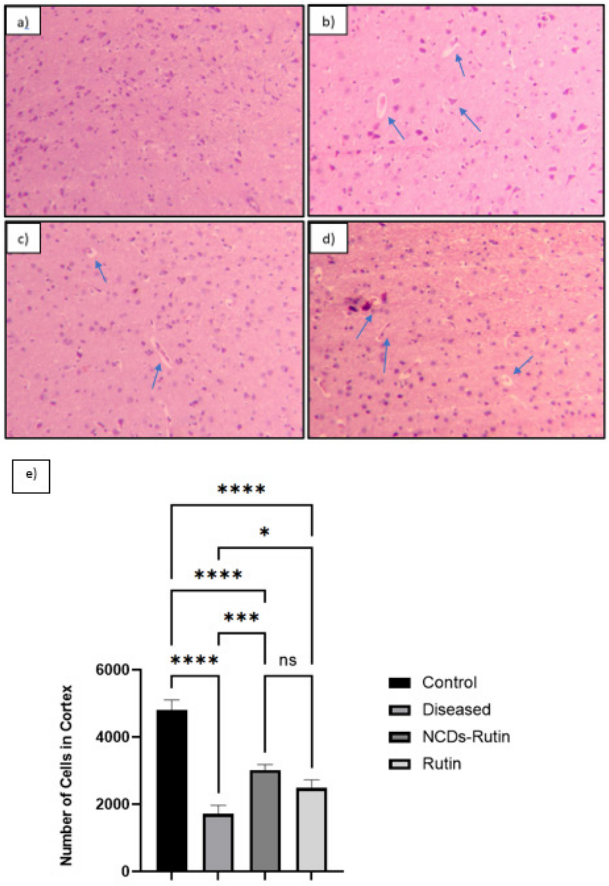

Figure 6. **Histopathological implications of NCDs-rutin treatment**: H & E-stained samples of diseased (**a**), healthy (**b**), NCDs-rutin treated (**c**), and rutin-treated (**d**) groups are depicted and the cell count is shown (**e**). Error bars present SEM (*p<0.05, ****p<0.0001). One-way ANOVA, followed by Tukey's multiple comparison tests, was used for statistical analysis of all the tests.

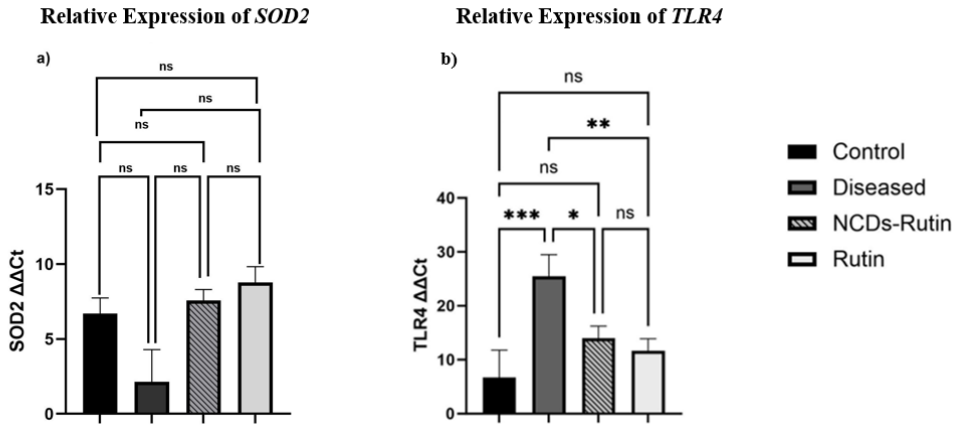

Figure 7. **ΔΔCt values after qPCR analysis**. The graphs depict ΔΔCt values of all the groups after qPCR analysis. NCDs-rutin and rutin administration normalized the expression levels of *SOD2* and *TLR4*. Error bars present SEM (*p<0.05, **p<0.01, ***p<0.001). One-way ANOVA, followed by Tukey's multiple comparison tests, was used for statistical analysis of all the tests.

sessment of rats, with a particular emphasis on the hippocampal-dependent aspects of learning and memory. Since the disease's pathology begins and is most prominent in these regions—the hippocampal and entorhinal cortex of the medial temporal lobe, these cognitive assessments are ideal for AD research [40]. MWM test evaluates spatial working memory and learning Y Maze test apparatus is a valuable tool for evaluating short-term spatial working memory, assessment of locomotor activity was conducted using a standard open field test, and to assess recognition memory, novel object recognition test was administered [41-43]. In the context of this study, rats were situated in an unfamiliar environment where they were initially allowed to move around freely and memorize the paths [43]. Previously, studies have shown rutin rescuing memory loss with high doses (100 mg/kg) for longer duration of time [44,45]. The current study yielded significant findings in the context that a single dose of NCDs-rutin was enough to mediate the effects similar to 30 doses of rutin. This study diminishes the dose and time taken to discern any visible change in cognitive impairment in rats.

Following behavioral assessments, tissues of the sacrificed rats were then used to assess the antioxidant parameters. *SOD2* is an essential biomarker that reflects the metabolic state of reactive oxygen species in the body. The amount of *SOD2* that is present can be used as a proxy for the organism's ability to eliminate free radicals; it is a critical component of immune defense against bacteria, pathogenic microbes, phagocytic cell activity, and malignant cells [46]. In a previous study, rutin's potential to enhance therapeutic outcomes has been explored against CTX-induced immune stress and oxidative damage. Study suggests rutin suppresses the cytokines TNF-α and IL-6 release and protects immune organs and increases *SOD2* content. Furthermore, they reveal that rutin regulates the expression levels of genes and proteins involved in the TLR4-MyD88-NF-*κ*B signaling pathway, which in turn affects immunological responses. These results imply that rutin has potential as a strong antioxidant and immunological stress regulator [46]. Comparably, in our study, qRT-PCR results depict that the expression levels of *SOD2* were shown to be down-regulated in the diseased group which was counter-affected by NCDs-rutin and rutin administration, more notable in the rutin-treated group. The *TLR4* gene expression levels were observed to be up-regulated due to $AlCl_3$. NCDs-rutin and rutin administration normalized the levels of *TLR4* with significant difference between the diseased and treated group. However, no significant difference was noted between the NCDs-rutin and rutin group. Although the results are nonsignificant, the pattern of regulation of *SOD2* and *TLR4* lies in line with the previous studies. The difference arises in the dose volume where a dose of 10 mg/kg of NCDs-rutin was administered whereas 50 mg/kg of rutin was administered to obtain the afore-mentioned results. Moreover, only a single dose of NCDs-rutin was given, while on the other hand, 30 doses of rutin were administered, which yielded similar affects.

The results indicate that NCDs-rutin functions as a more efficient and targeted approach to administering drugs for AD. The enhanced bioavailability and biocompatibility of the complex allows it to influence the target in shortened period of time. Despite knowing the exceptional properties of NCDs-rutin, several issues need to be resolved to direct their future applications. In particular, heightened focus should be placed on enhancing the optical performance of NCDs-rutin. To modify their optical characteristics, it is imperative to first synthesize a diverse range of NCDs with tunable compositions, sizes, forms, crystallinity, and electrical structures [22]. The utilization of animal models in evaluating cognitive impairment, though valuable, may fall short in replicating the full pathophysiology of AD in human subjects. The variability observed in species-specific responses and disease progression has the potential to significantly influence the interpretation of research findings.

It is also crucial to consider that the duration of the study conducted may have been insufficient to adequately evaluate the long-term therapeutic effects as well as the potential adverse reactions associated with NCDs-rutin. Therefore, it is imperative that extended follow-up periods be incorporated into future studies to assess the sustained efficacy and safety profile of NCDs-rutin over time. By addressing these identified limitations through the application of advanced methodologies and the implementation of comprehensive experimental designs, it is possible to enhance the robustness, reliability, and translational capacity of future investigations exploring the therapeutic potential of NCDs-rutin for AD.

CONCLUSION

In conclusion, the results of this study highlight the promising potential of NCDs-rutin as a novel therapeutic approach for AD. While the study is concentrated on characterizing the established complex, it is essential to obtain a comprehensive understanding of the molecular pathways involved. Future research endeavors should be directed towards conducting additional investigations in order to elucidate the complex signaling pathways and interactions responsible for the observed therapeutic outcomes. In this study, only *SOD2* was tested as an antioxidant parameter. Our future investigations will include testing for other markers of oxidative stress. Furthermore, the utilization of transgenic animal models that more accurately replicate AD pathology, such as APP/PS1, could improve the applicability and precision of preclinical

studies. These models display features like Aβ deposition and neuroinflammation that are reminiscent of human AD, offering valuable insights into the development of the disease and the effectiveness of therapeutic interventions.

Disclosure statement: Prior to or following the research project's start, none of the authors had any actual or potential conflicts regarding interests that might have improperly influenced their work. The authors of this paper have done this work impartially and objectively because they are dedicated to sustaining the highest level of scientific and academic quality.
Conflict of interest: The authors declare that no conflict of interest is associated with this study.

REFERENCES

1. Scheltens P, De Strooper B, Kivipelto M, Holstege H, Chételat G, Teunissen CE, et al. Alzheimer's disease. Lancet. 2021 Apr;397(10284):1577–90.
2. Schachter AS, Davis KL. Alzheimer's disease. Dialogues Clin Neurosci. 2000 Jun;2(2):91–100.
3. Selkoe DJ, Hardy J. The amyloid hypothesis of Alzheimer's disease at 25 years. EMBO Mol Med. 2016 Jun;8(6):595–608.
4. Busche MA, Hyman BT. Synergy between amyloid-β and tau in Alzheimer's disease. Nat Neurosci. 2020 Oct;23(10):1183–93.
5. Flynn JM, Melov S. SOD2 in mitochondrial dysfunction and neurodegeneration. Free Radic Biol Med. 2013 Sep;62:4–12.
6. Miao L, St Clair DK. Regulation of superoxide dismutase genes: implications in disease. Free Radic Biol Med. 2009 Aug;47(4):344–56.
7. Malik JA, Kaur G, Agrewala JN. Revolutionizing medicine with toll-like receptors: A path to strengthening cellular immunity. Int J Biol Macromol. 2023 Dec;253(Pt 7):127252.
8. Wu L, Xian X, Xu G, Tan Z, Dong F, Zhang M, et al. Toll-Like Receptor 4: A Promising Therapeutic Target for Alzheimer's Disease. Mediators Inflamm. 2022 Aug;2022:7924199.
9. De Vita T, Albani C, Realini N, Migliore M, Basit A, Ottonello G, et al. Inhibition of Serine Palmitoyltransferase by a Small Organic Molecule Promotes Neuronal Survival after Astrocyte Amyloid Beta 1-42 Injury. ACS Chem Neurosci. 2019 Mar;10(3):1627–35.
10. Sarrazin JL, Bonneville F, Martin-Blondel G. Brain infections. Diagn Interv Imaging. 2012 Jun;93(6):473–90.
11. Burgess A, Hynynen K. Drug delivery across the blood-brain barrier using focused ultrasound. Expert Opin Drug Deliv. 2014 May;11(5):711–21.
12. Zhou Y, Peng Z, Seven ES, Leblanc RM. Crossing the blood-brain barrier with nanoparticles. J Control Release. 2018 Jan;270:290–303.
13. Li S, Peng Z, Dallman J, Baker J, Othman AM, Blackwelder PL, et al. Crossing the blood-brain-barrier with transferrin conjugated carbon dots: A zebrafish model study. Colloids Surf B Biointerfaces. 2016 Sep;145:251–6.
14. Seven, E. S, Zhou, Y, Seven, Y. B, et al. Crossing Blood-Brain Barrier with Carbon Quantum Dots. The FASEB Journal. 2019;33(S1):785.8-785.8 https://doi.org/10.1096/fasebj.2019.33.1_supplement.785.8.
15. Zhou Y, Mintz KJ, Oztan CY, Hettiarachchi SD, Peng Z, Seven ES, et al. Embedding Carbon Dots in Superabsorbent Polymers for Additive Manufacturing. Polymers (Basel). 2018 Aug;10(8):921.
16. Zhang W, Sigdel G, Mintz KJ, Seven ES, Zhou Y, Wang C, et al. Carbon dots: A future blood–brain barrier penetrating nanomedicine and drug nanocarrier. Int J Nanomedicine. 2021 Jul;16:5003–16.
17. Ang-Lee MK, Moss J, Yuan CS. Herbal medicines and perioperative care. JAMA. 2001 Jul;286(2):208–16.
18. Awaad AS, El-Meligy RM, Qenawy SA, Atta AH, Soliman GA. Anti-inflammatory, antinociceptive and antipyretic effects of some desert plants. J Saudi Chem Soc. 2011;15(4):367–73.
19. Negahdari R, Bohlouli S, Sharifi S, Maleki Dizaj S, Rahbar Saadat Y, Khezri K, et al. Therapeutic benefits of rutin and its nanoformulations. Phytother Res. 2021 Apr;35(4):1719–38.
20. Nafees S, Mehdi SH, Zafaryab M, Zeya B, Sarwar T, Rizvi MA. Synergistic Interaction of Rutin and Silibinin on Human Colon Cancer Cell Line. Arch Med Res. 2018 May;49(4):226–34.
21. Gullón B, Lú-Chau TA, Moreira MT, Lema JM, Eibes G. Rutin: A review on extraction, identification and purification methods, biological activities and approaches to enhance its bioavailability. Trends Food Sci Technol. 2017 Sep;67:220–35.
22. Sharma S, Singh N, Nepovimova E, Korabecny J, Kuca K, Satnami ML, et al. Interaction of synthesized nitrogen enriched graphene quantum dots with novel anti-Alzheimer's drugs: spectroscopic insights. J Biomol Struct Dyn. 2020 Apr;38(6):1822–37.
23. Tejwan N, Kundu M, Ghosh N, Chatterjee S, Sharma A, Abhishek Singh T, et al. Synthesis of green carbon dots as bioimaging agent and drug delivery system for enhanced antioxidant and antibacterial efficacy. Inorg Chem Commun. 2022;139:109317.
24. Yan C, Wang C, Shao X, Shu Q, Hu X, Guan P, et al. Dual-targeted carbon-dot-drugs nanoassemblies for modulating Alzheimer's related amyloid-β aggregation and inhibiting fungal infection. Mater Today Bio. 2021 Nov;12:100167.
25. Bazzari FH, Abdallah DM, El-Abhar HS. Chenodeoxycholic Acid Ameliorates $AlCl_3$-Induced Alzheimer's Disease Neurotoxicity and Cognitive Deterioration via Enhanced Insulin Signaling in Rats. Molecules. 2019 May;24(10):1992.
26. Takeuchi H, Iba M, Inoue H, Higuchi M, Takao K. Tsukita, et al. Mutant Human Tau Transgenic Mice Manifest Early Symptoms of Human Tauopathies with Dementia and Altered Sensorimotor Gating; 2011. p. 301S.
27. Zhang R, Xue G, Wang S, Zhang L, Shi C, Xie X. Novel object recognition as a facile behavior test for evaluating drug effects in AβPP/PS1 Alzheimer's disease mouse model. J Alzheimers Dis. 2012;31(4):801–12.
28. Feldman AT, Wolfe D. Tissue processing and hematoxylin

and eosin staining. Methods Mol Biol. 2014;1180:31–43.
29. Alturkistani HA, Tashkandi FM, Mohammedsaleh ZM. Histological Stains: A Literature Review and Case Study. Glob J Health Sci. 2015 Jun;8(3):72–9.
30. Guo L, Yan H, Yan L, Bai L, Niu S, Zhao Y. A hyperbranched polysiloxane containing carbon dots with near white light emission. Polym Chem. 2021;12(24):3582–91.
31. Dhiman A, Singh D, Fatima K, Zia G. Development of Rutin Ethosomes for Enhanced Skin Permeation. International Journal of Traditional Medicine and Applications. 2019;1(1):4–10.
32. Panhwar QK, Memon S. Synthesis, characterisation, and antioxidant study of Cr(III)-rutin complex. Chem Pap. 2014;68(5):614–23.
33. Choi J, Reipa V, Hitchins VM, Goering PL, Malinauskas RA. Physicochemical characterization and in vitro hemolysis evaluation of silver nanoparticles. Toxicol Sci. 2011 Sep;123(1):133–43.
34. Calabrese G, De Luca G, Nocito G, Rizzo MG, Lombardo SP, Chisari G, et al. Carbon Dots: An Innovative Tool for Drug Delivery in Brain Tumors. Int J Mol Sci. 2021 Oct;22(21):11783.
35. Wang R, Sun Y, Huang H, Wang L, Chen J, Shen W. Rutin, A Natural Flavonoid Protects PC12 Cells Against Sodium Nitroprusside-Induced Neurotoxicity Through Activating PI3K/Akt/mTOR and ERK1/2 Pathway. Neurochem Res. 2015 Sep;40(9):1945–53.
36. Yu XL, Li YN, Zhang H, Su YJ, Zhou WW, Zhang ZP, et al. Rutin inhibits amylin-induced neurocytotoxicity and oxidative stress. Food Funct. 2015 Oct;6(10):3296–306.
37. Kunjiappan S, Chowdhury R, Bhattacharjee C. Isolation and structural elucidation of flavonoids from aquatic fern Azolla microphylla and evaluation of free radical scavenging activity. Int J Pharm Pharm Sci. 2013;5:743–9.
38. Pinto D, Lameirão F, Delerue-Matos C, Rodrigues F, Costa P. Characterization and Stability of a Formulation Containing Antioxidants-Enriched Castanea sativa Shells Extract. Cosmetics. 2021;8(2):49.
39. Betzer O, Shilo M, Opochinsky R, Barnoy E, Motiei M, Okun E, et al. The effect of nanoparticle size on the ability to cross the blood-brain barrier: an in vivo study. Nanomedicine (Lond). 2017 Jul;12(13):1533–46.
40. Puzzo D, Lee L, Palmeri A, Calabrese G, Arancio O. Behavioral assays with mouse models of Alzheimer's disease: practical considerations and guidelines. Biochem Pharmacol. 2014 Apr;88(4):450–67.
41. Bromley-Brits K, Deng Y, Song W. Morris water maze test for learning and memory deficits in Alzheimer's disease model mice. J Vis Exp. 2011 Jul;2920(53).
42. Prieur EA, Jadavji NM. Assessing Spatial Working Memory Using the Spontaneous Alternation Y-maze Test in Aged Male Mice. Bio Protoc. 2019 Feb;9(3):e3162.
43. Cohen RM, Rezai-Zadeh K, Weitz TM, Rentsendorj A, Gate D, Spivak I, et al. A transgenic Alzheimer rat with plaques, tau pathology, behavioral impairment, oligomeric aβ, and frank neuronal loss. J Neurosci. 2013 Apr;33(15):6245–56.
44. Sun XY, Li LJ, Dong QX, Zhu J, Huang YR, Hou SJ, et al. Rutin prevents tau pathology and neuroinflammation in a mouse model of Alzheimer's disease. J Neuroinflammation. 2021 Jun;18(1):131.
45. Ramalingayya GV, Nampoothiri M, Nayak PG, Kishore A, Shenoy RR, Mallikarjuna Rao C, et al. Naringin and Rutin Alleviates Episodic Memory Deficits in Two Differentially Challenged Object Recognition Tasks. Pharmacogn Mag. 2016 Jan;12(45 Suppl 1):S63–70.
46. Lan Z, Wang H, Wang S, Zhu T, Ma S, Song Y, et al. Rutin protects against cyclophosphamide induced immunological stress by inhibiting TLR4-NF-κB-mediated inflammation and activating the Nrf2- mediated antioxidant responses. Pharmacol Res Mod Chin Med. 2022 Sep;4:100135.